Fuel 231 (2018) 45–52

Contents lists available at ScienceDirect

Fuel

journal homepage: www.elsevier.com/locate/fuel

Full Length Article

Benzene and toluene removal from synthetic automotive gasoline by mono and bicomponent adsorption process

Paula Mariana Stähelin[a], Alexsandra Valério[a], Selene Maria de Arruda Guelli Ulson de Souza[a], Adriano da Silva[a], José Alexandre Borges Valle[b], Antônio Augusto Ulson de Souza[a,*]

[a] Department of Chemical and Food Engineering, Federal University of Santa Catarina, P.O. Box 476, 88040-900 Florianopolis, SC, Brazil
[b] Department of Textile Engineering, Federal University of Santa Catarina, 89065-300 Blumenau, SC, Brazil

ARTICLE INFO

Keywords:
Adsorption
Benzene
Toluene
Gasoline
Activated carbon

ABSTRACT

The oil and gas industry produces derivatives with a high content of toxic components, which are already present in crude oil or can be generated during the refinery process, with a negative effect on human health. Thus, the objective of this work was to study benzene and toluene removal from synthetic gasoline, using coconut shell-based activated carbon (18 × 30 mesh) as adsorbent. From the results, in the monocomponent kinetics, 1.1 mmol/g of benzene and 1.8 mmol/g of toluene removal were obtained at room temperature. The influence of the initial contaminant concentration was evaluated and the adsorption kinetics equilibrium was reached up to 60 min. The maximum adsorption capacity obtained through the isotherms, for the monocomponent system was 2.05 mmol/g for benzene and 2.04 mmol/g for toluene; on the other hand, in the bicomponent system, the adsorption capacity for toluene (1.05 mmol/g) was higher than that of benzene (0.8 mmol/g) due to polarity and molar mass. In addition, for the bicomponent adsorption system, it was observed that the presence of two components reduced adsorption when compared to the monocomponent system. Thus, this process proved to be appropriate for benzene and toluene removal from automotive gasoline.

1. Introduction

Automotive gasoline is one of the major petroleum products, with continuous consumption increase. Gasoline is a complex mixture of volatile and flammable hydrocarbons, which naturally contains benzene, toluene, and xylene-BTX [1]. In this way, BTX is an important component present in the exhaust gases of cars, causing major adverse effects on the heart, lungs and the brain [2]. According to WHO [3] among the pollutants, benzene has been associated with a range of acute and long-term adverse health, and due to the liposoluble characteristic, is rapidly absorbed in the respiratory system, and about 50% of the total absorbed can be stored in fat tissues, such as the central nervous system [4]. Though respiratory and cardiovascular effects of these emissions are well identified, psychological and neurobiological complications of prolonged exposure to vehicle emissions remain unknown [2]. Thus, the development of technologies to reduce the amount of these compounds is necessary.

Adsorption is a separation process in which the components of the fluid phase (liquid or gas) are transferred to the solid surface (adsorbent) by mass transfer [5,6]. The adsorption process is a spontaneous phenomenon, which indicates that Gibb's free energy must be negative ($\Delta G < 0$) and the reduction of the system disorder, when the molecule is adsorbed, leads to an entropy decrease ($\Delta S < 0$) [7].

Thus, chemical, physical and biological methods have been used to remove organic components as benzene and toluene from aqueous effluents. In this sense, activated carbon is by far the most common adsorbent used in wastewater treatment, since, during adsorption, the pollutant is removed by accumulation at the interface between the activated carbon (absorbent) and the liquid phase [6–12]. Activated charcoal has been considered a promising technology for the control of toxic pollutants and recovery of chemicals, and can be manufactured from the carbonaceous material, peat, wood, or nutshells (i.e., coconut) [13]. The manufacturing process consists of two phases, carbonization, and activation. [13–15].

Under this scenario, this work contributes to the literature in the field of adsorption of toxic compounds from automotive gasoline. Then, with the main goal to reduce benzene and toluene contents, a synthetic automotive gasoline was used, and the adsorption capacity of the coconut shell-based activated carbon as adsorbent was studied.

* Corresponding author at: Department of Chemical and Food Engineering, Federal University of Santa Catarina, UFSC, 88040-900 Florianópolis, SC, Brazil.
E-mail address: antonio.augusto.souza@ufsc.br (A.A. Ulson de Souza).

https://doi.org/10.1016/j.fuel.2018.04.169
Received 13 September 2017; Received in revised form 27 April 2018; Accepted 28 April 2018
Available online 29 May 2018

2. Material and methods

2.1. Material

Isooctane (2,2,4-trimethylpentane, Macron Fine Chemicals, 99.8%, 114.3 g/mol). Benzene (Sigma Aldrich, 99.9%) and toluene (Sigma Aldrich, 99.9%) were used as adsorbates. In addition, sodium hydroxide (NaOH, Chromate, 98%), hydrochloric acid (HCl, Labsynth, 38%), sodium chloride (NaCl, Vetec, 99%), and ethanol (Lafan, 99.5, molar mass 46.1 g/mol) were used. For the gas chromatographic analysis, 1,2,3,4-tetrahydronaphthalene (Fluka, 98.5%, 132.2 g/mol) was used as the internal standard. The activated carbon (ACC adsorbent) with specifications 0.9–0.5 mm, 18x30 mesh, moisture content 0.85% (0.17%), volatile material 25.5% (0.06%), ash content 6.77% (0.31%), surface area 758 m^2/g, volume of pores 0.4 cm^3/g, and mean pore diameter 21 Å, obtained from coconut shell used as adsorbent, was donated by Carbomafra S.A.

2.2. Adsorbent preparation and characterization

Initially, the ACC adsorbent was washed 5 times with distilled water and then kept 24 h in the water, the process was repeated three times, and then the adsorbent was dried at 105 °C for 24 h. The pH and adsorbent zero point charge (pzc) was performed at pH range from 2.5 to 11 prepared using 0.01 M NaCl and 0.1 M HCl solution, 0.1 g of ACC adsorbent was kept on an orbital shaker (150 rpm) at room temperature for 24 h. The textural analyses were performed using BET methods (Brunauer, Emmett, and Teller) and BJH (Barrett, Joyner, and Halenda) in order to evaluate the surface area, pore volume and mean diameter pore. Finally, in order to obtain information about the topology and morphology of the adsorbent Scanning Electron Microscope (SEM) analysis was performed.

2.3. Study of adsorbent concentration

The influence of adsorbent concentration was evaluated at a concentration range from 10 to 200 g/L. The experiment was carried out in a monocomponent system for benzene and toluene at 113 mmol/L and 376 mmol/L, respectively using isooctane as solvent. The adsorption capacity at equilibrium (qe) was determined in duplicate (n = 2), as described by Hackbarth et al. (2014) and Luz et al. at 23 ± 2 °C, 110 rpm, pH 6.3 for 24 h.

2.4. Kinetic and adsorption isotherms

The adsorption kinetics was evaluated using 40 g/L of the adsorbent, two benzene concentrations (113 mmol/L and 68 mmol/L in isooctane), and three toluene concentrations (376 mmol/L, 188 mmol/L, and 56 mmol/L in isooctane). The adsorption kinetics were performed in a batch mode (erlenmeyer 125 mL), in an orbital shaker at 110 rpm, pH 6.30, 23 ± 2 °C for 24 h. In order to evaluate the contaminant removal, samples were collected periodically and analyzed by gas chromatography. For the bicomponent assay, a stock solution at 113 mmol/L benzene and 376 mmol/L of toluene in isooctane (commercial gasoline contents) was initially prepared. In order to determine the highest affinity to the ACC adsorbent, the system was evaluated under same initial concentrations of benzene and toluene (113 mmol/L).

The adsorption isotherms (Table 1) were performed in a batch mode (erlenmeyer 125 mL), in an orbital shaker at 180 rpm, pH 6.30, 23 ± 2 °C, 40 g/L with equilibrium time defined in the kinetic study. In all mono and bicomponent assays, samples were analyzed by CG in triplicate (n = 3) at the initial time (C0), before contact with the adsorbent, and at the equilibrium time (Ce). The removed contaminant per gram of adsorbent was calculated by mass conservation balance for batch mode (Eq. (1)) [6,16].

Table 1
Initial concentrations of benzene and toluene used in the monocomponent and bicomponent adsorption isotherm.

Monocomponent system		Bicomponent system		
Benzene C_o (mmol/L)	Toluene C_o (mmol/L)	C_o (mmol/L)	Benzene:toluene C_0 (% v/v)	
0	0	0	0	0
113	47	56	0.5	0.6
135	94	113	1.0	1.2
158	141	169	1.5	1.8
180	188	225	2.0	2.4
203	235	282	2.5	3.0
281	282	338	3.0	3.6
338	329	394	3.5	4.2
394	376	450	4.0	4.8
450	422	–	–	–

$$q_t = \frac{V}{W}(C_0 - C_t) \tag{1}$$

where q_t is the amount of contaminant adsorbed at time t (mmol/g adsorbent), V is the solution volume (L), W is the dry adsorbent (g), C_0 is the initial concentration of adsorbate in the liquid phase (mmol/L), and C_t is the adsorbate concentration in the liquid phase at time t (mmol/L).

The obtained results for the monocomponent assay after adsorption time (t, min) was fitted to the pseudo-first order Eq. (2) and pseudo-second order (Eq. (3)) models [16,17].

$$q_t = q_e[1 - exp(-k_{1,ads}t)] \tag{2}$$

where q_e is equilibrium adsorption capacity (mmol/g de adsorbent), $k_{1,ads}$ constant of the pseudo-first order model (1/min).

$$q_t = \frac{q_e^2 k_{2,ads} t}{1 + k_{2,ads} q_e t} \tag{3}$$

where $k_{2,ads}$ is pseudo-second order constant (1/min).

The experimental results of the equilibrium assays were fitted to Langmuir (Eq. (4)), Freundlich (Eq. (5)), and Langmuir-Freundlich (Eq. (6)) models as shown in Fig. 5. The isotherm parameters are shown in Table 3.

$$q_e = \frac{q_L K_L C_e}{1 + K_L C_e} \tag{4}$$

where q_L is the maximum adsorption capacity (mmol/g), K_L is the constant related to the adsorbent affinity to the adsorbate (L/mmol), and C_e is the adsorbate concentration in the liquid phase in the equilibrium (mmol/L).

$$q_e = K_F (C_e)^{(\frac{1}{n})} \tag{5}$$

where K_F is the indicator of adsorption capacity ($mmol^{1-1/n}L^{1/n}$/g) and n is the Freundlich empirical parameter.

$$q_e = \frac{q_{LF} K_{LF} (C_e)^{(\frac{1}{n})}}{1 + K_{LF} (C_e)^{(\frac{1}{n})}} \tag{6}$$

where q_{LF} is the maximum adsorption capacity (mmol/g) and K_{LF} is the Langmuir-Freundlich constant.

The isotherm parameters, correlation coefficient (R^2), and benzene and toluene (RMSE) for the benzene and toluene were obtained by MatLab® software. The adsorption constants were obtained by non-linear regression analysis for each model as listed in Table 3 with the average percentage error. The RMSE was calculated by Eq. (7). The best-fitting models were identified based on the values of correlation coefficient and the best correlations are those with the highest values of R^2 lowest values for RMSE.

$$RMSE = \sqrt{\frac{\sum_{i=1}^{N} (q_{exp} - q_{cal})^2}{N}} \quad (7)$$

where subscripts exp and cal mean experimental and calculated values and N is the number of experiments.

2.5. Desorption and adsorbent reuse

After adsorption process, the adsorbent was filtered and dried at 40 °C for 60 min, and the desorption was performed using anhydrous ethanol. Three adsorption/desorption cycles were carried out in batch mode (110 rpm, 23 ± 2 °C, and 180 min) in order to evaluate the reuse capacity. Further, desorption tests at high temperatures to remove benzene and toluene from the ACC adsorbent was carried out. For this study, three adsorbent systems, two monocomponent and one bicomponent, at benzene and toluene concentrations of 113 mmol/L and 376 mmol/L, respectively, were evaluated. The desorption process was carried out in a muffle furnace at 300 °C for 90 min, then the ACC adsorbent was used in a new adsorption/desorption cycle.

2.6. Chromatographic analysis

Gas chromatography analyses (GC) were carried out in a Shimadzu GC-17A gas, with flame ionization detector (FID), column DB-5 (dimethylpolysiloxane, J&W Scientific, 30 m × 0.25 mm × 0.25 μm) using nitrogen as mobile phase. Chromatographic conditions: initial temperature 50 °C/5 min, heating rate 10 °C/min with final temperature at 200 °C column remained in this condition for 1 min. The temperature of the injector and detector was set at 200 °C and 250 °C, respectively. 1 μL of injected solution sample (split 1:50) was obtained. To correlate the output data of the equipment with the contaminant concentration and validate the method, analytical curves were determined for each compound, using the internal standardization method (internal standard added to the sample).

2.7. Statistic analysis

To determine the statistical difference in the precision of the kinetic and equilibrium models fitted to the experimental data, Test F was calculated according to Eq. (8) [18].

$$F_{cal} = \frac{S^2_{R(A)}}{S^2_{R(B)}} \quad (8)$$

where $S^2_{R(A)}$ and $S^2_{R(B)}$ are the residual variances of models A and B, respectively, the variance with higher R^2 is the denominator. The tabulated F value (F_{tab}) was determined at 95% of confidence level considering the degrees of freedom. If F calculated (F_{cal}) was lower than F_{tab}, there is no statistical difference between the models for the considered confidence level. On the other hand, if F_{cal} is higher than F_{tab}, the most precise model is the model with higher R^2.

3. Results and discussion

In this section, the characterization of the adsorbent, followed by the study of the adsorbent concentration, kinetics, isotherm, and desorption study will be presented. The results obtained for the adsorbent concentration were used in the kinetic study and isotherm determination.

3.1. Adsorbent characterization

From the zero point charge, pH 8 was the condition, which promoted the zero electrical charge density on ACC adsorbent surface indicating the basic character of the studied coconut shell-based activated carbon, showing that the adsorption can be higher in acid condition. As the initial pH of the benzene and toluene solution in isooctane was 6.30, it was considered favorable for the adsorption process. In the literature, some author also reported the basic characteristic for the coconut shell-based activated carbon [19–22]. Basic coconut shell-based activated carbon also shows hydrophobic characteristics favoring the adsorption of organic compounds, contributing to the lower moisture adsorption decreasing pores obstruction.

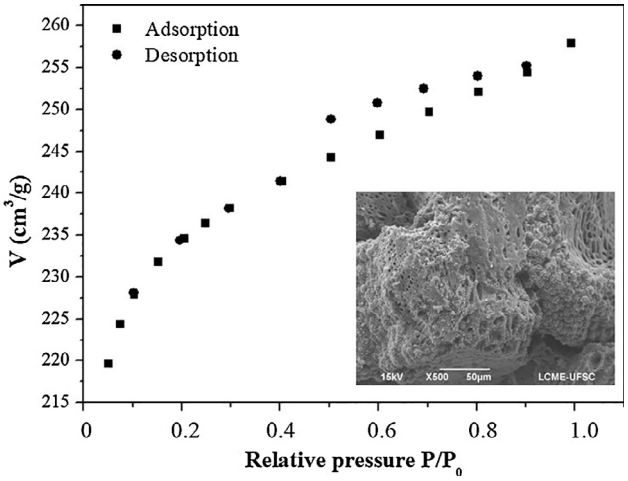

Fig. 1. Adsorption-desorption isotherm of N2 at 77 K for coconut shell-based activated carbon by BET method. SEM images of coconut shell-based activated carbon (right-hand side insert).

The BET assay (Fig. 1) showed the chemisorption process characterized by complete saturation of the monolayer at low equilibrium concentrations, characteristic to the solids microporous. However, a slight hysteresis between the adsorption and desorption curves was observed, which occurs when the gas evaporation inside the pores is different from the condensation process due to the plate-like particles aggregates forming slit-like pores or particles with irregular shape and broad pore size distribution. In addition (Fig. 1 right-hand side insert), SEM images showed irregular pore-filled surface on ACC adsorbent, with irregular shape and size. The fully pores surface can favor the adsorption process, by increasing the surface area of the adsorbent and increasing the number of active sites.

In addition, the adsorbent was found to have a BET surface area of 758.5 m^2/g, an average pore diameter of 21.1 Å, and total pore volume of 0.4 cm^3/g. Thus, BET and zero point charge allowed confirming the ACC adsorbent, studied in this work, as a good adsorbent for organic compounds, such as benzene and toluene.

3.2. Influence of adsorbent concentration on the contaminant removal

The influence of ACC adsorbent (coconut shell-based activated carbon) concentration was determined in a range from 10 to 200 g/L, resulting in a relation between adsorbed contaminant to ACC adsorbent concentration as shown for benzene (Fig. 2a) and toluene (Fig. 2b) due to the increase of available active sites. Thus, the results indicate that the adsorbent concentration had a positive influence on the benzene and toluene adsorption, and the adsorption capacity at equilibrium (q_e) was lower at higher adsorbent concentrations. From the obtained results, 40 g/L showed benzene (1.1 mmol/g (36%)) and toluene (1.8 mmol/g (16%)) removal, then, it was kept constant in the next steps of this work.

Increasing the adsorbent concentration provided higher adsorption sites, leading to the higher contaminant removal, further increase in the adsorbent amount did not affect the removal efficiency due to the maximum equilibrium adsorption capacity. Akpomie et al. [23] reported that the increase in the percentage removal could be associated

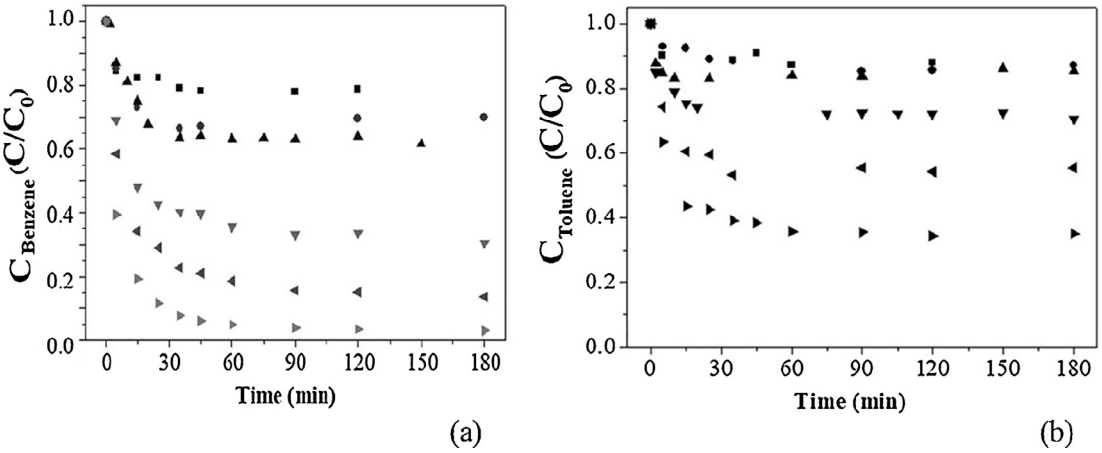

Fig. 2. Kinetics of benzene (a) and toluene (b) adsorption as a function of coconut shell-based activated carbon concentration (■) 10 g/L, (●) 20 g/L, (▲) 40 g/L, (▼) 80 g/L, (◄) 120 g/L, (►) 200 g/L. Conditions: $C_{0\ benzene}$ = 113 mmol/L, $C_{0\ toluene}$ = 376 mmol/L, 110 rpm, 24 h at 23 °C.

to the increase in the surface area and the availability of more active sites on the adsorbent surface. Similar results were reported by Azouaou et al., [16] for the cadmium adsorption in aqueous solution by coffee grounds, the authors reported an increased contaminant removal by increasing the adsorbent concentration, with maximum adsorption at 90%, due to saturation of the active sites.

3.3. Adsorption kinetics: Monocomponent system

Fig. 3 shows the kinetic curves of the pseudo-first and pseudo-second order used for the kinetics model fitting data related to the initial concentrations of benzene 110 mmol/L and 69 mmol/L (Fig. 3a) and toluene 376 mmol/L, 178 mmol/L, and 56 mmol/L (Fig. 3b). From the results, it was observed an increase in the contaminants adsorbed in the solid phase (qt) over time until the equilibrium be reached. The benzene kinetic curve showed a quick adsorption at the first stage reaching the equilibrium after 40 min. For toluene, a short equilibrium time was observed (up to 30 min). In addition, for benzene, it was not observed the increase of solute amount removed as a function of initial ACC concentration, as observed for toluene, where the effect was more evident.

The kinetic parameters for benzene (Fig. 3a) and toluene (Fig. 3b) obtained from the fitted curves are shown in Table 2. From the fitted data, at benzene initial concentration of 110 mmol/L, it was not verified statistical difference between the two models ($F_{tab} > F_{cal}$) at 95% of confidence. On the other hand, at 69 mmol/L, a statistical difference between the models was observed and the pseudo-second-order model was best to describe the adsorption of benzene (R^2 = 0.961). As well as, for the toluene experimental data, no statistical difference between the pseudo-first-order and pseudo-second order models at 376 mmol/L ($F_{tab} > F_{cal}$) was observed. However, at 178 and 56 mmol/L, statistical difference was observed and the pseudo-second order model described better the benzene adsorption Table 3.

Table 2
Pseudo-first-order and pseudo-second order model parameters for benzene and toluene adsorption by coconut shell-based activated carbon at different initial concentrations (mean ± standard deviation).

Benzene	C_0 (mmol/L)	q_e (mmol/g)	k (g/mg·min)	R^2
Pseudo-first order	110	1.09 ± 0.02	0.08 ± 0.01	0.987
	69	0.98 ± 0.04	0.15 ± 0.03	0.890
Pseudo-second order	110	1.26 ± 0.06	0.07 ± 0.02	0.967
	69	1.05 ± 0.03	0.24 ± 0.05	0.961
Toluene	C_0 (mmol/L)	q_e (mmol/g)	k (g/mg·min)	R^2
Pseudo-first order	376	1.77 ± 0.03	0.48 ± 0.06	0.980
	178	1.49 ± 0.06	0.16 ± 0.02	0.972
	56	0.74 ± 0.02	0.07 ± 0.01	0.970
Pseudo-second order	376	1.84 ± 0.01	0.48 ± 0.04	0.996
	178	1.59 ± 0.02	0.16 ± 0.01	0.992
	56	0.82 ± 0.03	0.12 ± 0.05	0.994

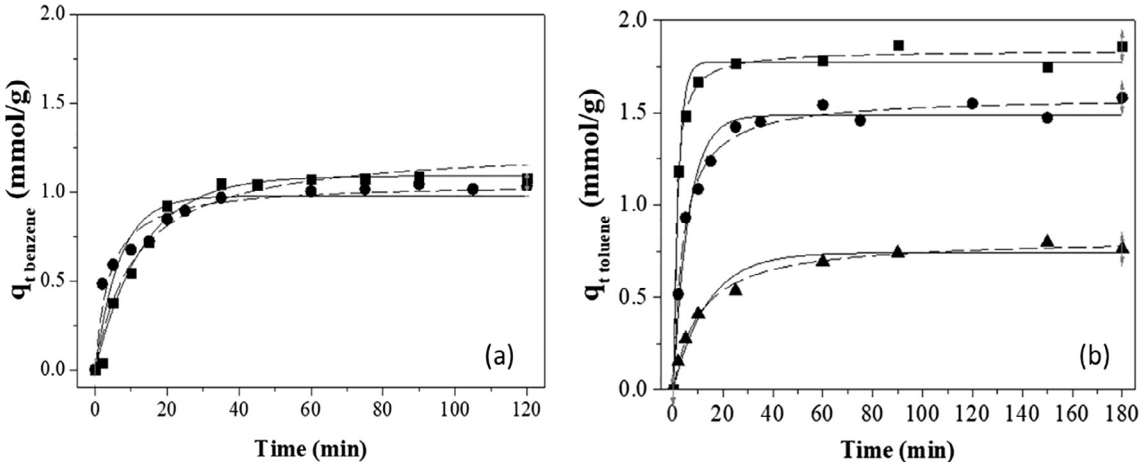

Fig. 3. Kinetic curves of benzene adsorption (a) at initial concentrations of 110 mmol/L (■) and 69 mmol/L (●), and kinetic curves of toluene adsorption (b) at initial concentrations of 376 mmol/L (■), 178 mmol/L (●), and 56 mmol/L (▲). Adjustment to pseudo-first order (solid line) and pseudo-second order (dash line) models. Conditions: $C_{adsorbent}$ 40 g/L, 110 rpm at 23 °C.

Table 3
Langmuir, Freundlich, and Langmuir-Freundlich isotherm parameters for benzene and toluene monocomponent adsorption (mean ± standard deviation).

Isotherms	Parameter	Benzene	Toluene
Langmuir	q_L (mmol/g)	2.21 ± 0.21	1.66 ± 0.13
	K_L (L/mmol)	0.011 ± 0.003	0.020 ± 0.006
	R^2	0.955	0.954
	RMSE	0.133	0.100
Freundlich	n	2.98 ± 0.57	3.11 ± 0.32
	K_F ($mmol^{1-1/n}L^{1/n}/g$)	0.25 ± 0.09	0.24 ± 0.04
	R^2	0.961	0.983
	RMSE	0.112	0.063
Langmuir-Freundlich	q_{LF} (mmol/g)	2.21 ± 1.25	1.66 ± 0.43
	K_{LF} (L/g)	0.014 ± 0055	0.037 ± 0.046
	n_{LF}	1.03 ± 1.19	1.15 ± 0.60
	R^2	0.955	0.957
	RMSE	0.117	0.099

One of the most important conclusions from the kinetics study, as previously verified, was that for all benzene and toluene initial concentrations, the equilibrium was reached up to 60 min, indicating the saturation of the active sites available that contributed to fast removal of adsorbate molecules, with over time, the number of vacant active sites reduced and removal was observed to decrease. Similar results were observed by Zheng et al., [24], Azouaou et al., [16], and Carvalho et al., [6]. Even that the adsorption equilibrium reached up to 60 min for benzene and toluene, in order to ensure the equilibrium and the contact time between the ACC adsorbent and the adsorbate solution, for the next experiments, the reaction time was fixed in 180 min.

3.4. Adsorption kinetics: Bicomponent system

Fig. 4 shows the mono and bicomponent adsorption curves of benzene (113 mmol/L) and toluene (376 mmol/L). By comparing the results, it was concluded that in the monocomponent adsorption, benzene had a higher removal but in a slower rate, while in the bicomponent system 19% of benzene was adsorbed for the monocomponent system 36% was adsorbed.

This result can be justified by the competitive adsorption by the active sites in the bicomponent adsorption between benzene and toluene. In addition, it was observed the preference for the toluene adsorption. Thus, in order to better compare the bicomponent adsorption, a system with the same toluene and benzene initial concentration (113 mmol/L) was evaluated, and in this case, a similar removal for both contaminates was observed, however, a preference for the toluene (28%) adsorption compared to the benzene (22%) was once again observed.

3.5. Adsorption isotherm: Monocomponent system

Adsorption is a well-known equilibrium separation process for wastewater treatment and the equilibrium data, commonly known as adsorption isotherms, are basic requirements for the design of adsorption systems and provide information on the capacity of the adsorbent or the amount required to remove a unit mass of pollutant under the system conditions [5,7]. Based on R^2 and RMSE, Freundlich best-fitted isotherm to the experimental data for benzene and toluene. For toluene, a statistical difference between Langmuir and Freundlich models and Langmuir and Langmuir-Freundlich was observed, but no statistical difference between Freundlich and Langmuir-Freundlich models was observed.

Freundlich equation is based on the heterogeneous multilayer surfaces adsorption, where the adsorption sites have different affinities for the adsorbate and the sites with the highest attractive forces are first occupied [6,9,25]. For both evaluated compounds, the adsorption process was a favorable phenomenon, with n values between 1 and 10. Values above 10 indicate a non-reversible adsorption isotherm behavior. However, this equation does not provide any information about the maximum adsorption capacity. In the Langmuir isotherm, on the other hand, it was assumed that adsorption occurs at specific homogeneous internal sites and there is no significant interaction between the adsorbate, in this case, the adsorbent is saturated after a layer of adsorbed molecules formed on the adsorbent surface [10].

In this work, Langmuir-type isotherms have shown maximum adsorption capacity of 2.21 mmol/g for benzene and 1.66 mmol/g for toluene. The results reported in this work were compared to the results related to the literature (Table 4). By comparing the results, it was possible to be noted that for the monocomponent system, the maximum adsorption capacity for benzene was slightly higher than that reported for toluene. Thus, even though the solvent used in this study was isooctane and not water (with a different influence on the solubility), the behavior in terms of adsorption capacity was similar to that reported in the literature.

3.6. Adsorption isotherms: Bicomponent system

Fig. 6a and b shows the monocomponent and bicomponent isotherms for benzene and toluene, respectively. From the results, it was verified that in the bicomponent isotherms the maximum adsorption capacity, for both systems, were lower compared to the monocomponent system, showing a competitive adsorption for the active site of the adsorbent. Therefore, from the thermodynamic equilibrium tests,

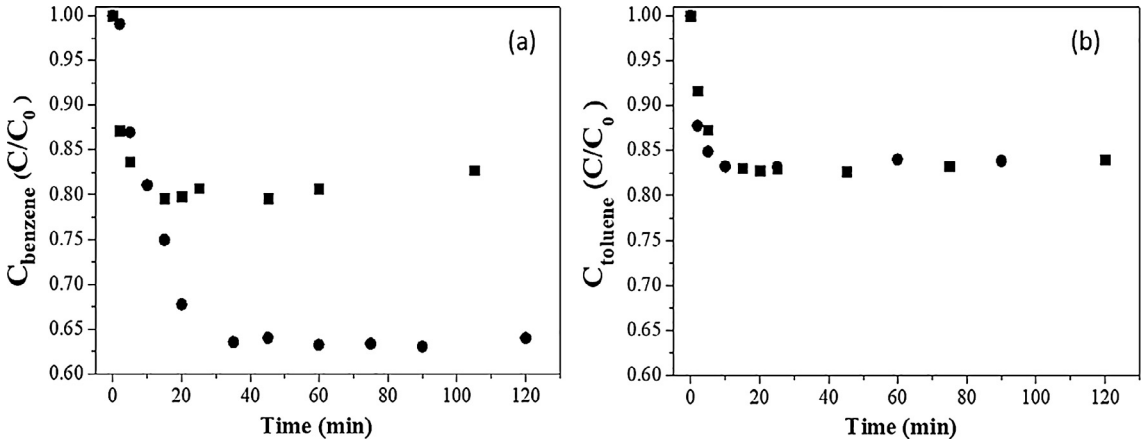

Fig. 4. Monocomponent (●) and bicomponent (■) adsorption for benzene (a) and toluene (b) at C_0 benzene 113 mmol/L, C_0 toluene 376 mmol/L, $C_{adsorbent}$ 40 g/L, 110 rpm at 23 °C.

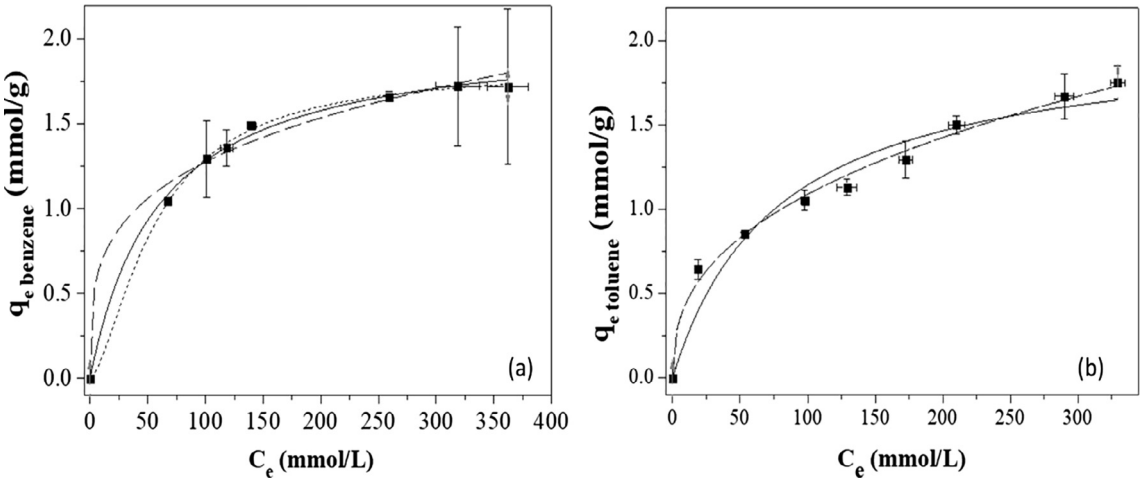

Fig. 5. Monocomponent adsorption isotherm for benzene (a) and toluene (b) by coconut shell-based activated carbon at 23 °C, $C_{adsorbent}$ 40 g/L, and 110 rpm. Experimental data (■) adjustment to Langmuir (solid line) Freundlich (dash line), Langmuir-Freundlich (dot line) models.

it was possible to notice that for the monocomponent systems the maximum adsorption capacity for benzene and toluene was similar. In addition, it was observed the preference of ACC adsorbent for the toluene (1.05 mmol/g) compared to benzene (0.8 mmol/g).

Studies related to the BTX removal from aqueous effluents also indicate the adsorbent affinity for the toluene in relation to benzene [4,6,8,26]. Thus, in general, the solubility of the solute in the solvent also reduces the adsorption process [8]. Another important point to be considered is the polarity, as the ACC adsorbent has an apolar characteristic, a higher affinity by the toluene will be noticed once toluene is more apolar than benzene [5,8].

3.7. Study of the desorption and reuse cycles

For benzene, in the first desorption cycle (Fig. 7a), 50% of desorption efficiency was observed, followed by 80% and 87% in the second and thirty cycles, respectively. On the other hand, for toluene (Fig. 7b), at first adsorption cycle, 75% of desorption efficiency was observed, reaching 100% in the third cycle. The desorption capacity was appropriated, even decreasing along the cycles, related to the cumulative amount of adsorbate remaining in the solid after treatment cycles, since the desorption process was not complete.

After monocomponent desorption study, the bicomponent system (Fig. 7c) was evaluated, at 113 mmol/L of benzene and 376 mmol/L of toluene. For bicomponent adsorption/desorption cycle, it was observed that the percentage of contaminant desorbed in the first cycle was lower (34% of recovery for benzene and 46% for toluene) compared to the monocomponent study. The reduction on the desorption efficiency can be related to the competitive by the adsorbent active sites. The desorption was also effective in the subsequent cycles reaching a desorption efficiency of 95% for toluene and 73% for benzene.

Fig. 7d shows the benzene and toluene removed in the adsorption/desorption cycles using high temperature as the recovery agent. For both compounds, it can be concluded that the desorption using muffle was quite efficient since, in the second and third cycles, the adsorbed amount was slightly lower than the adsorbed in the first cycle reaching values up to 95%.

Therefore, both desorption processes, using solvent or high temperature, proved to be efficient under the conditions evaluated in this work. The heating process is more aggressive and, therefore, promoted higher desorption in relation to the solvent process, however, it should be emphasized that during the choice of the adsorbent recovery method is important to evaluate the peculiarity of each process.

Table 4
Maximum adsorption capacity of different adsorbents obtained from the literature for the monocomponent system.

Adsorbent	Maximum adsorption capacity (mmol/g)		pH	T (°C)	(rpm)	Refs.
	Benzene	Toluene				
Coconut shell-based activated carbon	1.47	1.36	6.4	23	120	[24]
Coconut shell-based activated carbon	0.65	0.68	7.2	26	150	[13]
Granular activated carbon	2.35	2.11	7.0	30	–	[25]
Powdered activated carbon	0.51	0.43	–	–	–	[26]
PEG-Montmorillonite	0.08	0.07	7.0	25	250	[15]
Montmorillonite	0.36	0.29	–	–	–	[26]
Thermally modified diatomite	0.004	0.003	–	20	–	[23]
Zeolite	0.35	0.22	–	–	–	[26]
Zeolite Y with HDTMA surfactant	1.93	1.65	–	28	300	[7]
Zeolite Na-P1	1.86	8.13	–	–	–	[2]
Zeolite Na-P1 with HDTMA	6.22	9.27	–	–	–	[2]
Resin purolite-macronet MN-202	0.8	0.7	5.4	26	150	[13]
Claytone-40	0.17	0.17	6.4	26	150	[13]
Smectite clay with HDTMA	0.007	0.007	9.0	23	300	[4]
Mesoporous silica with gallium incorporated	4.48	4.47	–	25	200	[6]
Carbon nanotubes modified with NaOCl	2.95	2.74	7.0	25	180	[26]
Coconut shell-based activated carbon	2.05	2.04	6.3	23	110	Present work

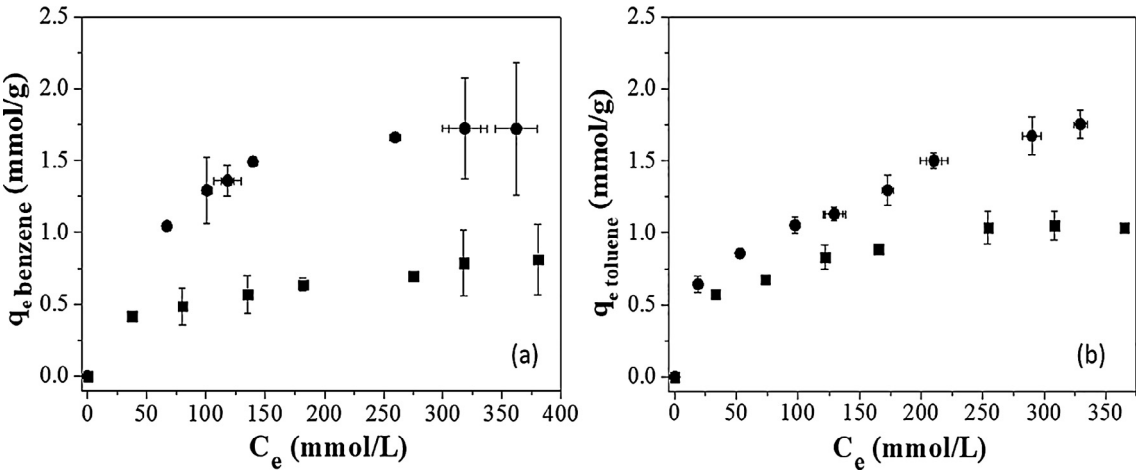

Fig. 6. Monocomponent (●) and bicomponent (■) adsorption isotherm for benzene (a) and toluene (b) by coconut shell-based activated carbon at 23 °C, $C_{adsorbent}$ 40 g/L, and 110 rpm.

4. Conclusion

The characterizations of coconut shell-based activated carbon used as the adsorbent in this study indicate a very porous structure with a higher surface area, favoring the adsorption process. In addition, the basic characteristic verified, highlight the adsorption of organic compounds in slightly acidic solutions. The mono- and bicomponent adsorption kinetics achieved the equilibrium adsorption capacity up to 60 min, which can favor an industrial scale process, using fixed bed columns in series, for example, until complete contaminant removal. From the study of the initial contaminant concentrations was observed that when a higher initial benzene or toluene concentration was used a higher *qe* was obtained. In relation to the fitted models to the kinetic data, the pseudo-second order model showed the best fitting with no significant statistical difference. In the bicomponent kinetics, at same benzene and toluene initial concentrations (113 mmol/L), a removal of

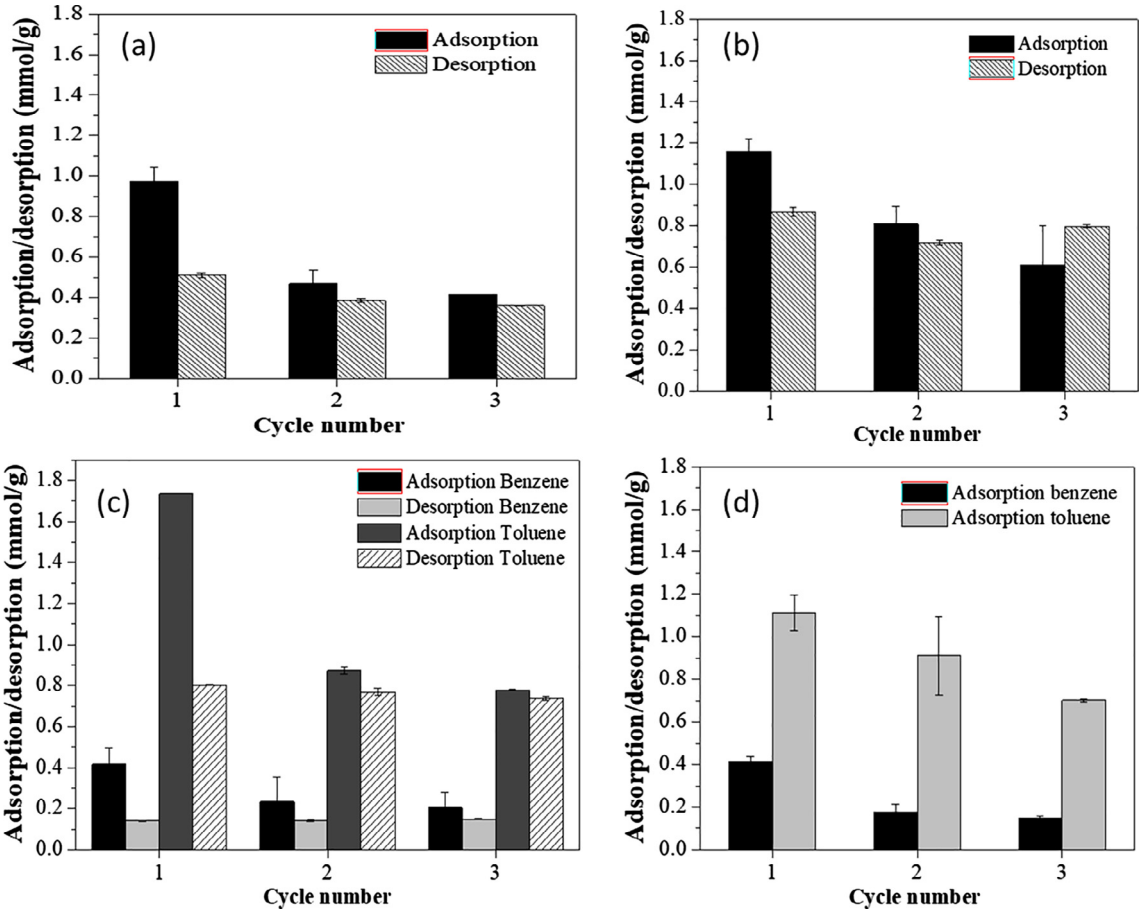

Fig. 7. Monocomponent benzene (a) and toluene (b) removal, and bicomponent benzene-toluene (c) in the adsorption/desorption cycles using ethanol as the solvent in the desorption process, and monocomponent system using high temperature in the desorption process (d). Conditions: $C_{0\ benzene}$ 94 mmol/L, $C_{0\ toluene}$ 343 mmol/L, $C_{adsorbent}$ 40 g/L, 110 rpm, 180 min, at 23 °C.

22% for benzene and 28% for toluene, indicated the preference for toluene adsorption. In the isotherm adsorption study, it was related that in the benzene monocomponent system, Langmuir-Freundlich model best described the monolayer adsorption, and for the toluene monocomponent system, Freundlich model best describes the monolayer adsorption. However, in the bicomponent system, toluene's higher affinity to the coconut shell-based activated carbon was observed with adsorption at 1.05 mmol/g, while for benzene the adsorption was 0.8 mmol/g, attributed to the polarity and molar mass of the compounds.

Acknowledgments

The author thank financial support from ANP – Brazil (National Petroleum Agency) through the ANP Human Resources Program for the Oil and Natural Gas – Brazil Sector ANP-MME/MCT – Brazil-PRH 09.

References

[1] Correa SM, Arbilla G, Marques MRC, Oliveira KMPG. The impact of BTEX emissions from gas stations into the atmosphere. Atmos Pollut Res 2012;3:163–9. http://dx.doi.org/10.5094/APR.2012.016.
[2] Salvi A, Patki G, Liu H, Salim S. Psychological impact of vehicle exhaust exposure: insights from an animal model. Sci Rep 2017;7:8306. http://dx.doi.org/10.1038/s41598-017-08859-1.
[3] World Health Organization. Benzene. In: Air quality guidelines for Europe, 2nd ed. Copenhagen: 2000.
[4] Szala B, Bajda T, Matusik J, Zięba K, Kijak B. BTX sorption on Na-P1 organo-zeolite as a process controlled by the amount of adsorbed HDTMA. Micropor Mesopor Mater 2015;202:115–23. http://dx.doi.org/10.1016/j.micromeso.2014.09.033.
[5] McCABE WL, SMITH JC, HARRIOTT P. Unit operations of chemical engineering. (5th ed.) New York: McGraw-Hill; 1993.
[6] Carvalho MN, da Motta M, Benachour M, Sales DCS, Abreu CAM. Evaluation of BTEX and phenol removal from aqueous solution by multi-solute adsorption onto smectite organoclay. J Hazard Mater 2012;239–240:95–101. http://dx.doi.org/10.1016/j.jhazmat.2012.07.057.
[7] Ruthven DM. Principles of adsorption and adsorption processes. (3rd ed.) New York: New York: John Wiley & Sons, Inc.; 1984.
[8] Prabhu A, Shoaibi A Al, Srinivasakannan C. Development of gallium incorporated mesoporous silica catalysts for the selective removal of BTX. Appl Catal A Gen 2013;466:137–41. http://dx.doi.org/10.1016/j.apcata.2013.06.050.
[9] Vidal CB, Raulino GSC, Barros AL, Lima ACA, Ribeiro JP, Pires MJR, et al. BTEX removal from aqueous solutions by HDTMA-modified Y zeolite. J Environ Manage 2012;112:178–85. http://dx.doi.org/10.1016/j.jenvman.2012.07.026.
[10] Moura CP, Vidal CB, Barros AL, Costa LS, Vasconcellos LCG, Dias FS, et al. Adsorption of BTX (benzene, toluene, o-xylene, and p-xylene) from aqueous solutions by modified periodic mesoporous organosilica. J Colloid Interface Sci 2011;363:626–34. http://dx.doi.org/10.1016/j.jcis.2011.07.054.
[11] Daifullah AA, Girgis B. Impact of surface characteristics of activated carbon on adsorption of BTEX. Coll Surf A Physicochem Eng Asp 2003;214:181–93. http://dx.doi.org/10.1016/S0927-7757(02)00392-8.
[12] Li Y, Gupta G. Adsorption of hydrocarbons by clay minerals from gasoline. J Hazard Mater 1994;38:105–12. http://dx.doi.org/10.1016/0304-3894(94)00006-9.
[13] Zheng C, Zhao L, Zhou X, Fu Z, Li A. Treatment technologies for organic wastewater. water treat. InTech 2013. http://dx.doi.org/10.5772/52665.
[14] Eibner S, Margeriat A, Broust F, Laurenti D, Geantet C, Julbe A, et al. Catalytic deoxygenation of model compounds from flash pyrolysis of lignocellulosic biomass over activated charcoal-based catalysts. Appl Catal B Environ 2017;219:517–25. http://dx.doi.org/10.1016/j.apcatb.2017.07.071.
[15] Mor S, Chhoden K, Negi P, Ravindra K. Utilization of nano-alumina and activated charcoal for phosphate removal from wastewater. Environ Nanotechnol, Monit Manage 2017;7:15–23. http://dx.doi.org/10.1016/j.enmm.2016.11.006.
[16] Azouaou N, Sadaoui Z, Djaafri A, Mokaddem H. Adsorption of cadmium from aqueous solution onto untreated coffee grounds: Equilibrium, kinetics and thermodynamics. J Hazard Mater 2010;184:126–34. http://dx.doi.org/10.1016/j.jhazmat.2010.08.014.
[17] Seifi L, Torabian A, Kazemian H, Bidhendi GN, Azimi AA, Farhadi F, et al. Kinetic study of BTEX removal using granulated surfactant-modified natural zeolites nanoparticles. Water, Air, Soil Pollut 2011;219:443–57. http://dx.doi.org/10.1007/s11270-010-0719-z.
[18] Miller JN, Miller JC. Statistics and chemometrics for analytical chemistry. 6th London: Pearson; 2010.
[19] Montes-Morán MA. The Basicity of Carbons. In: Elsevier O, editor. Tascón Nov. Carbon Adsorbents; 2012, p. 173–203.
[20] Fuente E, Menéndez JA, Suárez D, Montes-Morán MA. Basic surface oxides on carbon materials: a global view. Langmuir 2003;19:3505–11. http://dx.doi.org/10.1021/la026778a.
[21] Souza C, Majuste D, Ciminelli VST. Effects of surface properties of activated carbon on the adsorption mechanism of copper cyanocomplexes. Hydrometallurgy 2014;142:1–11. http://dx.doi.org/10.1016/j.hydromet.2013.11.003.
[22] Xing L, Xie Y, Cao H, Minakata D, Zhang Y, Crittenden JC. Activated carbon-enhanced ozonation of oxalate attributed to HO oxidation in bulk solution and surface oxidation: effects of the type and number of basic sites. Chem Eng J 2014;245:71–9. http://dx.doi.org/10.1016/j.cej.2014.01.104.
[23] Akpomie KG, Dawodu FA, Adebowale KO. Mechanism on the sorption of heavy metals from binary-solution by a low cost montmorillonite and its desorption potential. Alexandria Eng J 2015;54:757–67. http://dx.doi.org/10.1016/j.aej.2015.03.025.
[24] Zheng W, Li X, Yang Q, Zeng G, Shen X, Zhang Y, et al. Adsorption of Cd(II) and Cu (II) from aqueous solution by carbonate hydroxylapatite derived from eggshell waste. J Hazard Mater 2007;147:534–9. http://dx.doi.org/10.1016/j.jhazmat.2007.01.048.
[25] Aivalioti M, Vamvasakis I, Gidarakos E. BTEX and MTBE adsorption onto raw and thermally modified diatomite. J Hazard Mater 2010;178:136–43. http://dx.doi.org/10.1016/j.jhazmat.2010.01.053.
[26] Lu C, Su F, Hu S. Surface modification of carbon nanotubes for enhancing BTEX adsorption from aqueous solutions. Appl Surf Sci 2008;254:7035–41. http://dx.doi.org/10.1016/j.apsusc.2008.05.282.